Original article

Exogenous Indian hedgehog antagonist damages intervertebral discs homeostasis in adult mice

Ran Chen [a,1], Ya Tan [b,1], Yang Li [a,1], Junlan Huang [c], Liang Kuang [c], Zhenhong Ni [c], Haiyang Lan [d], Rui Long [e], Yangli Xie [c], Hangang Chen [c], Xiaoqing Luo [c], Lin Chen [c], Ying Tang [a,e,**], Siru Zhou [a,*]

[a] War Trauma Medical Center, State Key Laboratory of Trauma, Burns and Combined Injury, Army Medical Center, Daping Hospital, Army Medical University, Chongqing, 40038, People's Republic of China
[b] Department of Hematology, Southwest Hospital, First Affiliated Hospital of the Army Medical University, Chongqing, 40038, People's Republic of China
[c] Department of Wound Repair and Rehabilitation Medicine, State Key Laboratory of Trauma, Burns and Combined Injury, Trauma Center, Research Institute of Surgery, Daping Hospital, Army Medical University, Chongqing, 40038, People's Republic of China
[d] Department of Orthopedics, Army Medical Center, Daping Hospital, Army Medical University, Chongqing, 40038, People's Republic of China
[e] Department of Emergence Medicine, Army Medical Center, Daping Hospital, Army Medical University, Chongqing, 40038, People's Republic of China

ARTICLE INFO

ABSTRACT

Background: Vismodegib, as an exogenous Indian hedgehog (Ihh) antagonist, has been approved by the Food and Drug Administration (FDA) for the clinical treatment of patients with basal cell carcinoma, and previous observations implicate the potential therapeutic of vismodegib in osteoarthritis treatment. However, there is no direct evidence for the role of Ihh signaling in intervertebral discs (IVDs) homeostasis of adult mice. The aim of the present study is to assess the effect of systemic administration of Smoothened inhibitor (SMOi) - vismodegib on IVDs homeostasis during the adult stage.

Methods: The expression of glioma-associated oncogene homolog 1 (Gli1), the downstream targeting gene of Ihh signaling, in IVDs of adult mice after receiving systemic administration of SMOi was examined by immunohistochemistry. The pathological changes of vertebral bodies after SMOi treatment were evaluated by X-ray and micro-CT. The effects of SMOi on homeostasis of IVDs including cartilaginous endplates (CEP), growth plates (GP) and annulus fibrous (AF) were evaluated by histological analysis. The expressions of Aggrecan, Matrix metalloproteinase 13 (MMP13) and Runt-related transcription factor 2 (Runx2), in IVDs were also investigated by immunohistochemistry. Changes in chondrocyte apoptosis and proliferation in IVDs were evaluated by terminal deoxynucleotidyl transferase dUTP nick-end labeling (TUNEL) assay and analyzing the expression of the cell proliferation antigen Ki-67.

Results: Systemic administration of SMOi significantly decreased the expression of Gli1 in IVDs that indicating effective inhibition of Ihh signaling. Bone mass of vertebral bodies was diminished after SMOi treatment. Moreover, IVDs degeneration (IDD) like defects including CEP sclerosis, degenerative nucleus pulposus (NP) and fissure within AF, as well as narrowed or fused GP and loss bone mass of vertebral bodies was observed in SMOi-treated mice. The severity of IDD was time-dependent with the administration of SMOi treatment after 2–8 weeks. The expressions of Aggrecan, MMP13 and Runx2 in IVDs of mice receiving SMOi treatment were significantly decreased. In addition, chondrocyte apoptosis was significantly enhanced, while chondrocyte proliferation was significantly inhibited.

Conclusions: Our study propose that systemic administration of vismodegib damages IVDs homeostasis via inhibition of Ihh signaling in adult mice. The clinical application of Ihh signaling antagonists such as vismodegib should be careful considering these side adverse.

The Translational Potential of this Article: Vismodegib as an exogenous antagonist of Ihh signaling has been approved by the FDA for the clinical treatment of patients with basal cell carcinoma. However, it is still unknown whether vismodegib will has adverse effects on the patient or animal model of IVDs cartilage homeostasis. Based

on our study, systemic administration of vismodegib damages IVDs homeostasis via inhibition of Ihh signaling in adult mice and special attention should be paid to the clinical application of vismodegib.

1. Introduction

Low back pain (LBP) is a major musculoskeletal disorder causing disability in the worldwide. Intervertebral discs (IVDs) are complex cartilaginous tissue, and IVDs degeneration (IDD) is an important reason of LBP [1]. IDD is characterized by nucleus pulposus (NP) loss, annulus fibrosus (AF) defects and cartilaginous endplates (CEP) sclerosis or calcification [2]. Various molecules and pathways involved in cartilage development and degeneration, such as hedgehog (Hh) signaling pathway, are implicated in the pathogenesis of IDD and able to potentially serve as therapeutic targets [3,4].

In the canonical Hh signaling pathway, Hh family includes three homologues, Indian Hh (Ihh), Sonic Hh and Desert Hh [5]. The activation and transduction of the Ihh signaling pathway require the participation of a variety of signaling molecules, in which the Ihh ligand binds to Patched receptor and releases Smoothened (Smo), thus activating nuclear transcription factors the glioma-associated oncogene homolog (Gli) family and causing biological effects [6] (Fig. 8A and B). Ihh signaling is a critical pathway to regulate the skeletal development and homeostasis during the postnatal stage, especially in endochondral ossification. In the development of the GP, Ihh is mainly expressed in the pre-hypertrophic zone and in a few chondrocytes in hypertrophic zone, which directly regulates the proliferation and hypertrophy of chondrocytes [7,8]. During human osteoarthritis (OA) development, activation of Ihh signaling promotes the expression of OA markers, such as type-X collagen and matrix metalloproteinase (MMP) −13 for chondrocyte hypertrophy that closely associated with cartilage degeneration [9]. Inhibition of Ihh signaling attenuates cartilage degradation by suppressing chondrocyte hypertrophy in post-traumatic OA mouse models of the knee joint and temporomandibular joint (TMJ) [10], whereas activation of Ihh signaling in turn leads to OA in normal knee joints [11,12]. These evidences indicate that Ihh signaling is a therapeutic target for OA, and inhibition of Ihh signaling in the articular cartilage may prevent or delay OA progression in adults.

Previous works indicated that the pathophysiological process of IDD resembles OA. For example, both the hypertrophic differentiation of chondrocytes and the degradation of cartilage matrix are common characteristics that are observed in these pathological process [13]. Furthermore, similar to articular cartilage, Ihh is synthesized and expressed in the postnatal IVDs and Ihh signaling plays a significant role in growth, differentiation and aging of IVDs [3,14], and the blockade of Ihh signaling via knockdown Ihh with siRNA suppresses the expression of cartilage degeneration markers both *in vitro* and *ex vivo* [15]. These evidences speculate that Ihh signaling may also serve as a therapeutic target to modify IDDs progression *in vivo*. What is noteworthy is that Hh signaling pathway is essential for the embryonic formation and postnatal homeostasis of IVDs, in which Shh contributes to the synthesis of extracellular matrix and maintenance of IVDs structure and function in adults [6]. Additionally, our previous observations suggested that Ihh signaling inhibitor could play a role as "double-edged sword", *i.e.*, it inhibited chondrocytes hypertrophy while also suppressed proliferation of chondrocytes in TMJ cartilage during the adult stage, especially in health cartilage [16], and similar results were also reported in following study by other research groups [17]. Therefore, it is necessary to investigate the effect of inhibitor in Ihh signaling on the health IVDs during adult stages *in vivo*.

The ligands and receptors such as Smo and Gli1 in Ihh signaling are generally considered as the common targets for pharmacologic agents [18]. Vismodegib (GDC-0449), a selective inhibitor of Smo (SMOi), is an exogenous antagonist of Ihh signaling that has been discovered in recent years, and has been widely used in various cancers preclinical models

dependent on Ihh signaling pathway [18] (Fig. 8A and B). These studies clearly support the potential of vismodegib to regulate several cancer-related cellular processes via inhibition of Ihh signaling pathway, including proliferation, migration, invasion and angiogenesis [5]. Moreover, due to satisfied clinical remission rate in basal cell carcinoma, vismodegib has been approved by the FDA for the clinical treatment of patients with basal cell carcinoma [18]. However, it is still unknown whether vismodegib will has adverse effects on the patient or animal model of IVDs cartilage homeostasis. Considering that Ihh signaling is essential for the embryonic formation and postnatal homeostasis of IVDs [6] and vismodegib is already being used in clinical patients, this question is required to be clear. Therefore, it is necessary to investigate the effect of vismodegib on health IVDs during the adult stage *in vivo*.

In order to determine whether vismodegib mediated Ihh signaling pathway blockade has an impact on IVDs cartilage homeostasis, systemic delivery of vismodegib in adult mice was investigated in the present study. Our results demonstrated that inhibition of Ihh signaling by SMOi treatment resulted in IDD-like changes, including CEP sclerosis, degenerative NP and fissure within AF, as well as narrowed or fused GP and diminished bone mass of vertebral bodies. Based on these findings, we propose that systemic administration of vismodegib damages IVDs homeostasis in adult mice.

2. Materials and methods

2.1. Ethical statement

All mice were of the C3H/HeJ background. Animal studies were performed in strict accordance with protocols approved by the Laboratory Animal Welfare and Ethics Committee of Army Medical center (Chongqing, China).

2.2. Animals and groups

As reported in our previous study, vismodegib was reconstituted in 50% (w/v) 2-hydroxypropyl-β-cyclodextrin (Sigma-Aldrich, St. Louis, MO, USA) in sterile water for intraperitoneal injection in mice [16]. In present study, eighty male mice in adult (8 weeks, 25–30 g) were randomly divided into eight groups: mice in the SMOi groups were intraperitoneally injected with vismodegib (0.5 mg/day/10 g body weigh) daily for 3 days (SMOi_3-days group, n = 10), 2-weeks (SMOi_2-weeks group, n = 10), 4-weeks (SMOi_4-weeks group, n = 10) and 8-weeks (SMOi_8-weeks group, n = 10), respectively; The remaining mice served as controls and were injected with the same amount of 50% (w/v) 2-hydroxypropyl-β-cyclodextrin (Sigma-Aldrich, St. Louis, MO, USA) in sterile water for 3 days, 2, 4 and 8 weeks, respectively. After the completion of time course (3 days, 2, 4, or 8 weeks), the mice in SMOi and control groups were sacrificed after the breeding 1 day and sampled. The schedule of administration of SMOi and vehicle control in mice is shown in Fig. 1A. Up to the end of this study, none of mice in this study has died and other signs of systemic adverse events unexpectedly during SMOi or vehicle control injection.

2.3. X-ray and micro-computed tomography scanning and analysis

The IVDs specimens were placed on the workbench and exposed for 15s and X-ray images were obtained using an MX-20 Cabinet X-ray system (Faxitron X-Ray, Tucson, AZ, USA). The each undecalcified lumbar vertebrae was scanned using a vivaCT 40 micro-CT system (Scanco Medical, Brüttisellen, Switzerland) with an isotropic voxel size of 15 μm. Constant thresholds (222) were applied to grayscale images to
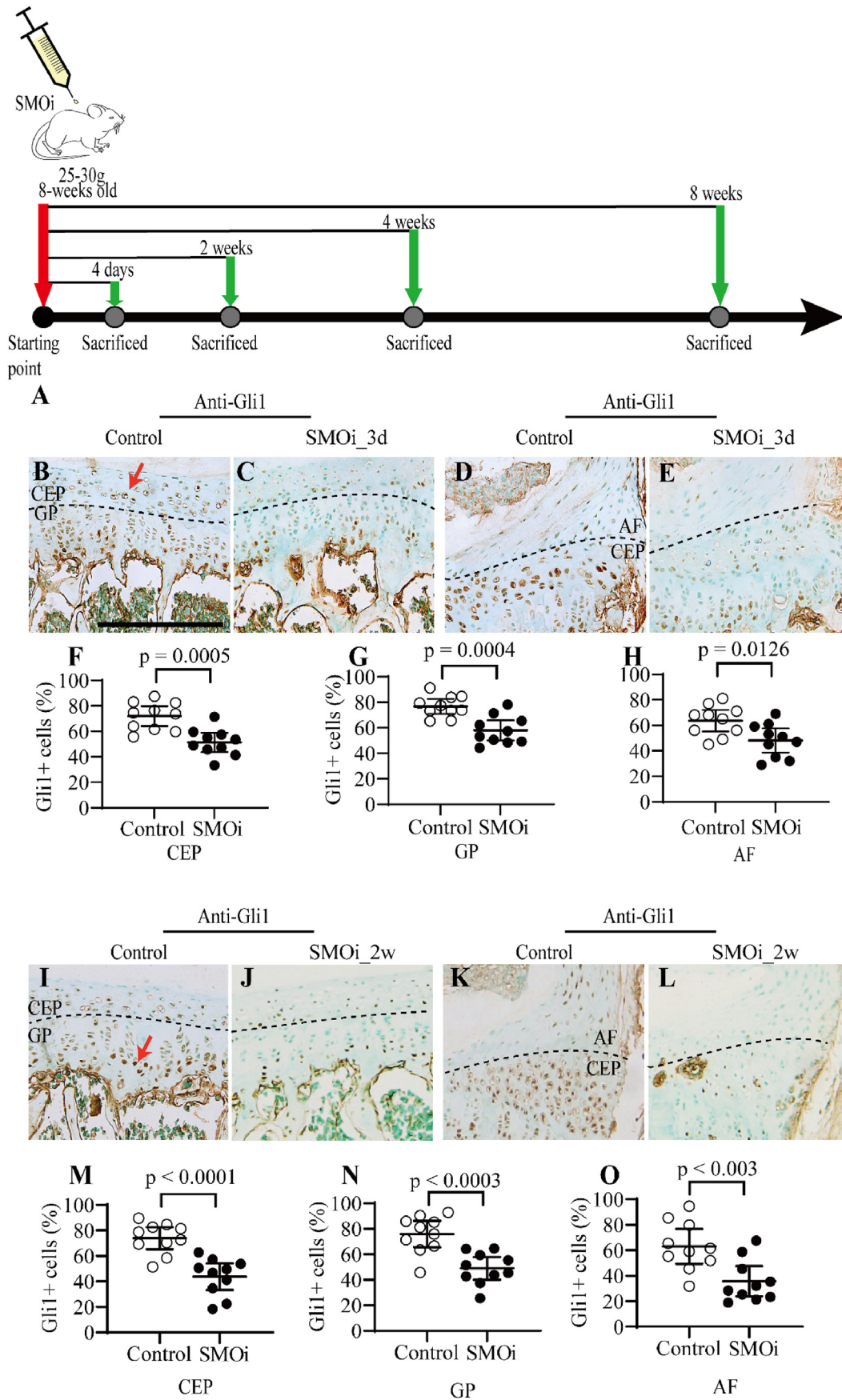
(caption on next page)

Figure 1. Systemic delivery of SMOi inhibits Ihh signaling activation in IVDs tissue of mice. **(A)** Scheme of experiment showing that mice in SMOi groups received daily intraperitoneal injection of SMOi for 3 days, 2, 4, and 8 weeks, respectively, and control vehicle mice received the same amount of 50% (W/V) 2-hydroxypropyl-β-cyclodextrin and sterile water. After the completion of time course, mice were sacrificed after the breeding 1 day and sampled. **(B–H)** Immunohistochemistry assay for Gli1 expression in IVDs of mice treated SMOi for 3 days. The Gli1-positive cells in CEP **(B, C, F)**, GP **(B, C, G)** and AF **(D, E, H)** in SMOi and control groups. **(I–O)** Immunohistochemistry assay for Gli1 expression in IVDs of mice treated SMOi for 2 weeks. The Gli1-positive cells in CEP **(I, J, M)**, GP **(I, J, N)** and AF **(K, L, O)** in SMOi and control groups. Red arrows: positive cells. GP: growth plates, CEP: cartilaginous endplates, AF: annulus fibrosus, SMOi: smoothened inhibitor, vismodegib. Values represent mean with 95%CI. *p < 0.05. (n = 10), Scale bar: 500 μm.

distinguish the bone from soft tissues. A cylindrical volume of interests (VOIs) was selected for three-dimensional (3D) reconstructions, which were in central trabeculae bone between the superior and inferior cartilage endplates of the L4 vertebral bodies in the all groups (a total of 120 images were scanned in each IVDs specimens). The microstructural indices of volume of interests (L4), bone volume/tissue volume (BV/TV) was collected. Serial 15-μm 2-D and 3-D images were acquired at 70 kV and 113 mA.

2.4. Histological assessment

Lumbar IVDs samples were fixed in 4% paraformaldehyde in 0.1 M phosphate buffer overnight, decalcified in 15% EDTA-phosphate buffered saline at 4 °C for 10 days and then embedded in paraffin. 5-μm thick sections were stained with Alcian blue combined with hematoxylin and eosin (H & E) for light microscopic examination. These stained sections were used to investigate the degenerative change scoring of IVDs (L4/5) using a modified scoring system [19,20]. The scoring system integrated classification system proposed by Melgoza et al. for evaluating age-related characteristics of the lumbar IVDs based on degenerative alteration of CEP, NP and AF [21].

2.5. Immunostaining analysis

Decalcified lumbar vertebral sections were deparaffinized with xylene for 30 min, and endogenous peroxidase activity was quenched by treatment with 3% H_2O_2 for 10 min, followed by antigen retrieval by trypsinization for 10 min at 37 °C. Sections were then blocked with normal goat serum for 30 min and incubated at 4 °C overnight with primary antibody followed by the appropriate biotinylated secondary antibody and horseradish peroxidase-conjugated streptavidin-biotin staining. Immunoreactivity was visualized with a 3,3′-diaminobenzidine tetrahydrochloride kit (ZSGB-BIO, Beijing, China) followed by counterstaining with Methyl Green. Primary antibodies against the following proteins were used: Ki-67 (1:100; Abcam, Cambridge, MA, USA), MMP-13 (1:200; Abcam, Cambridge, MA, USA), Aggrecan (1:100; Abcam, Cambridge, MA, USA Abcam), Gli1 (1:100, Abcam, Cambridge, MA, USA) encoding runt-related transcription factor-2 (Runx2), (1:100; Abcam, Cambridge, MA, USA). According to the instructions for each type of antibody, cells with hyperchromatic nuclei or cytoplasm are selected as positive cells. Ten paraffin sections in each group were randomly selected to observe the same area including GP, AF and CEP under an optical microscope and the number of positive cells was calculated using Image J (Rawak Software Inc., Stuttgart, Germany).

2.6. Apoptosis assay

The TUNEL assay was carried out with the In Situ Cell Death Detection kit (Roche Applied Science, Pleasanton, CA, USA) according to the manufacturer's instructions. According to the instructions, cells with green fluorescence are selected as positive cells. Ten paraffin sections in each group were randomly selected to observe the same area at CEP, NP and GP under the fluorescence microscope and the number of positive cells was calculated using Image J (Rawak Software Inc., Stuttgart, Germany).

2.7. Statistical analysis

Data were analyzed using the SPSS 19.0 software (SPSS Inc., Chicago, IL, USA) and GraphPad Prism v.9.0 software (GraphPad Inc., La Jolla, CA, USA). Results in our graphs were expressed as mean with 95% confidence interval. Differences between 2 groups were evaluated using Unpaired Student's t test. Analysis of variance (ANOVA) was used for comparisons of multiple groups followed by Tukey post hoc test. P < 0.05 was considered statistically significant.

3. Results

3.1. Systemic delivery of SMOi inhibits Ihh signaling activation in IVDs tissue of mice

Among Ihh signaling pathway, three Gli isoforms including Gli1, Gli2 and Gli3 in mammals are the downstream effector of Smo. Gli1 is not only the transcription activator but also as a transcriptional protein of GLI2, thereby amplifying the transcriptional response to Hh signals [22, 23]. Moreover, Gli1 is able to directly induce cellular differentiation in a Runx2-independent manner and mediates the biological function of Gli2 and Gli3 in osteogenesis [24] and Gli1 is typically thought to be a reliable biomarker of Ihh signaling activation [25]. To investigate the inhibiting effect of Ihh signaling after SMOi treatment in IVDs tissue, the expression of Gli1 were assessed in IVDs of mice that received daily injection of SMOi or vehicle control intraperitoneally for 3 days. Immunohistochemistry (IHC) analysis for Gli1 expression in IVDs tissues showed that a large number of positive cells located in CEP, GP and AF of control IVDs (Fig. 1B and D), and which was significantly decreased by 28.54%, 24.43% and 24.37% in CEP, GP and AF after SMOi treatment (Fig. 1C, E and F–H). Further analysis of X-ray, micro-CT, histological stain showed that there was no significant difference in vertebral bones and IVDs structural integrity between mice treated with SMOi for 3 days and control groups (Fig. 1S). These data demonstrated that SMOi treatment directly inhibited Ihh signaling in IVDs tissues after daily administration for 3 days.

While the expression of Gli1 in IVDs was further reduced in mice after treated with SMOi for 2 weeks. Statistical analysis showed that the proportion of cells expressing Gli1 in IVDs of SMOi group was significantly decreased by 40.86%, 35.37% and 43.36% in CEP, GP and AF, respectively (Fig. 1I-O). Moreover, obvious changes such as bone cavities within the CEP were observed (Fig. 1L). Together, these data suggested that Ihh signaling in the IVDs of SMOi group was further inhibited after 2-weeks SMOi treatment and induce morphological change in IVDs.

3.2. SMOi treatment causes loss volume of spinal bone mass in mice

Ihh signaling is closely involved in osteoblastic activity and the regulation of bone remodeling [26]. Further study found that Ihh is expressed at the osteogenic edge of growing cranial bones, and promotes bone formation by regulating osteogenic differentiation [27]. To investigate the effect of Ihh signaling inhibition on the bone quality and gross change of spine in mice during the adult stage, X-Ray assessment was performed. The imaging analysis showed that central trabecular structure within the vertebral body was slightly reduced, while trabecular spacing was increased in mice that received SMOi treatment for 2 weeks compared to vehicle control groups (Fig. 2A and B). These changes were obvious gradually in mice that had been injected with SMOi for 4 and 8
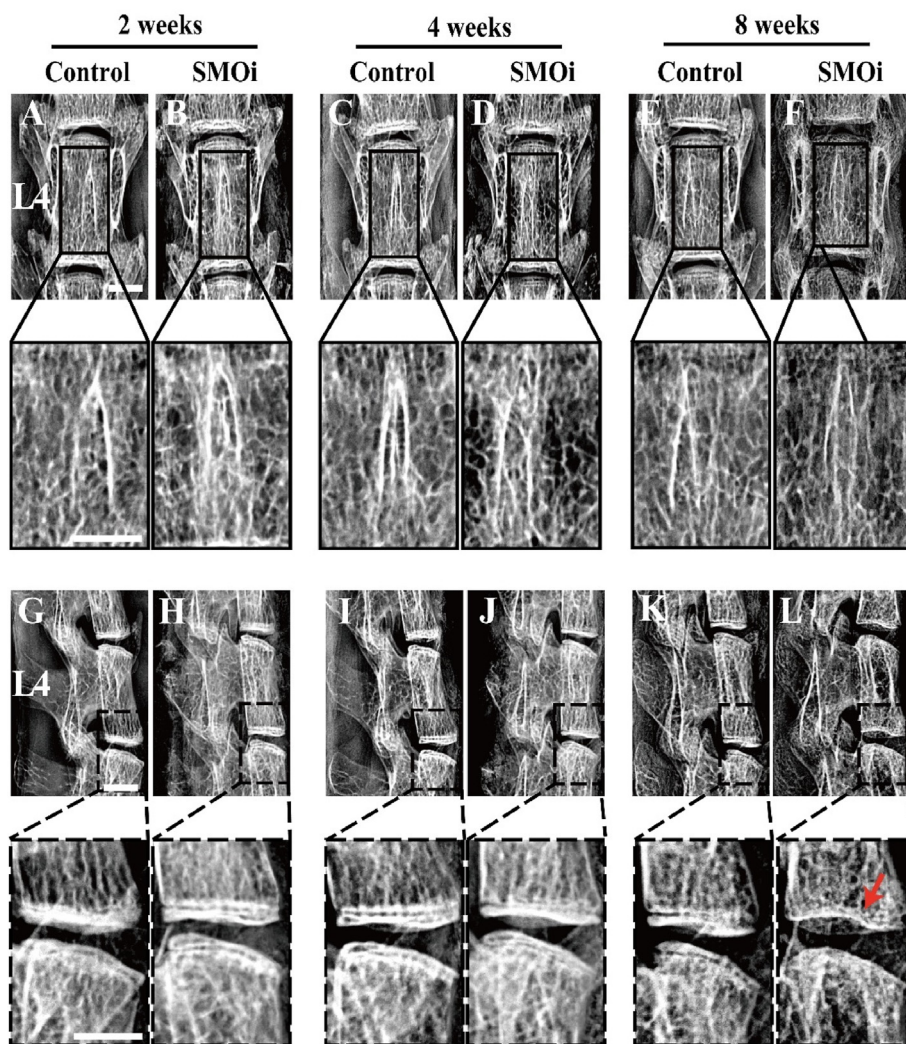
Figure 2. Radiographic assessment of lumbar spine phenotypes in mice. (A-L) The film of spines of mice that received SMOi injection and vehicle control treatment and higher magnification views of L4 and L4/5 IVDs in solid and dotted boxes. Red arrows: fusion of CEP, IVDs: intervertebral discs, SMOi: smoothened inhibitor, vismodegib, L4: the 4th lumbar., Scale bar: 1000 μm.

weeks (Fig. 2C–F) and the X-ray images also showed that CEP and GP at the end of intervertebral bodies fused after 8 weeks of continuous SMOi injection (Fig. 2L, Red arrow).

Furthermore, 3D reconstruction images indicated that the trabecular number and thickness of the cancellous bone in the vertebral body is gradually decreased with following SMOi injection for 2, 4 and 8 weeks (Fig. 3A–F). CT parametric analysis confirmed these changes and a gradual decrease in bone volume fraction (BV/TV) after SMOi injection, which reached a statistically significant difference after 8-weeks SMOi injection (Fig. 3G). These results indicated that systemic delivery of SMOi caused the decrease of vertebral bone volume in adult mice.

3.3. Systemic delivery of SMOi leads IDD-like changes in mice

Histological analyses were carried out to focus on the morphological and cellular changes underlying in IVDs of these mice. In control groups at different time points, chondrocytes in the proliferative zone of GP displayed a typical columnar organization and CEP connecting IVDs to the vertebrae was almost uniform in thickness and filled with round chondrocytes and extracellular matrix (Fig. 4A, C and E). AF showed normal organization of fibrocartilage lamellae and the NP contained abundant hydrated inner structure and cells sounded by large zones of acellular matrix (4A, C and E).

However, during the course of SMOi treatment, a series of IDD-like changes appeared in the IVDs of mice. First of all, the volume of the GP began to decrease and a clear reduction in the zone of proliferating chondrocytes with an irregular organization were observed (Fig. 4B). These phenotypes became more obvious at 4 weeks after SMOi injection and GP notably becomes further narrowed and even lost their normal structural continuity after 8 weeks of SMOi treatment (Fig. 4B, D and F). Secondly, a number of bone cavities within the CEP, especially located in the outer CEP border were observed in mice after 2 weeks SMOi treatment (Fig. 4B). These cavities became more obvious and began to appear gradually in the center of the CEP after 4 and 8 weeks of SMOi treatment in mice (Fig. 4D and F), which is consistent with previous study and represents a symbol of CEP sclerosis [28,29]. Thirdly, SMOi treatment resulted in the disorganization with obvious fissures in fibrocartilage lamellae of AF (Fig. 4B, D and F). Last but not the least, vacuolation of NP cells and loss of extracellular matrix, as main characteristics of IDD [2], which were obvious especially in SMOi groups at 8 weeks of SMOi treatment compared with the control group (Fig. 4B, D and F). Since GP, CEP, NP and AF of the IVDs in mice all showed varying degrees of degeneration after SMOi systemic injection, a histologic assessment of IDD degeneration was applied to evaluate the pathological changes in IVDs [21]. Statistical analysis revealed that there was a significant increase in total scores of IDD in SMOi group, which indicated that IDD
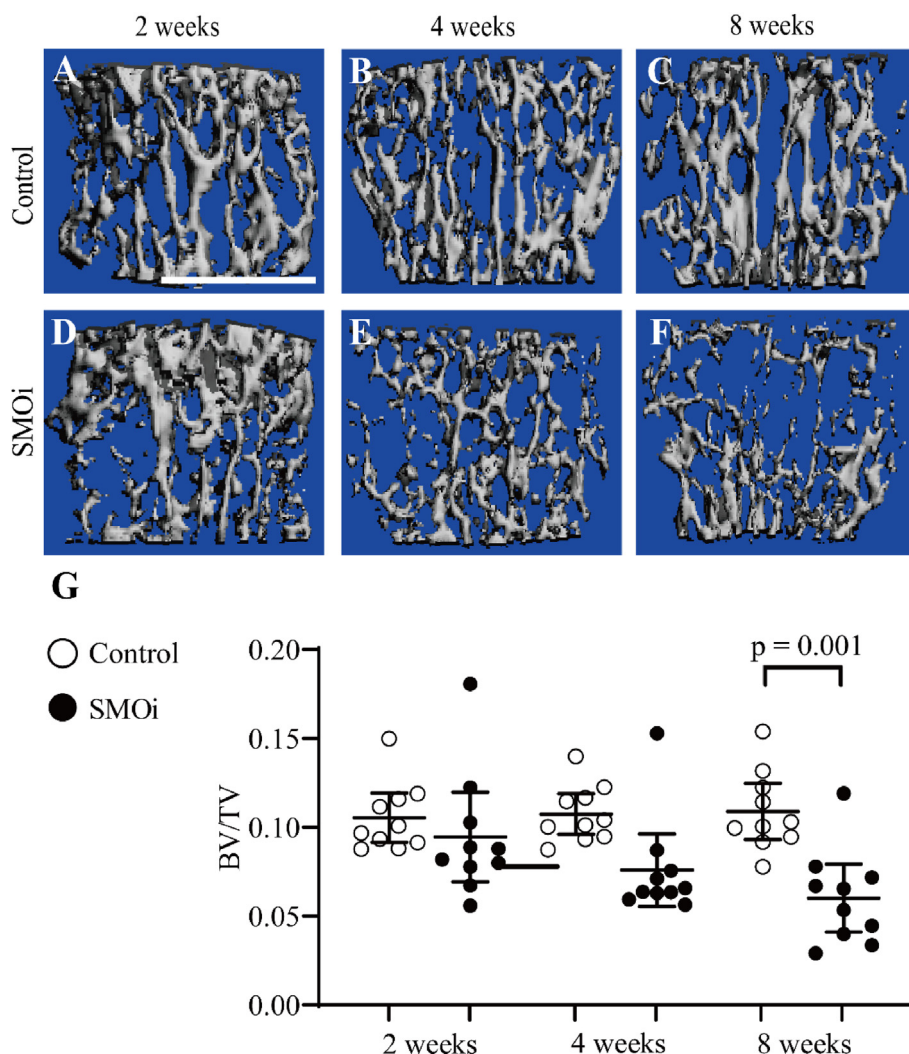
Figure 3. Micro-CT analysis of L4 in mice. (A-F) The 3D reconstruction of central bone trabecular structure of L4 bodies in SMOi and control groups. (**G**) The BV/TV in L4 in the SMOi and control groups. SMOi: smoothened inhibitor, vismodegib. Values represent mean with 95%CI. *$p < 0.05$, (n = 10), Scale bar: 1000 μm.

occurred in the IVDs of mice in the SMOi group (Fig. 4G). Therefore, these results indicated that systemic delivery of SMOi treatment caused IDD-like changes in mice.

3.4. Systemic delivery of SMOi impairs the homeostasis of cartilage in mice IVDs

Due to the early phenotype of IDD-like changes was observed in the IVDs of mice after 2-weeks SMOi treatment, we select this timepoint to further investigate the pathological alterations and underlying mechanism. Aggrecan is a proteoglycan with many glycosaminoglycan side chains located in the cartilage of IVDs, and the loss of proteoglycan expression in cartilage is supposed as an early event in IDD [30]. IHC staining for aggrecan showed that positive cells were significantly decreased in CEP of mice after SMOi treatment compared to that in the vehicle control group (Fig. 5A, B and E). Considering the less organization of AF was observed in SMOi-treated mice, we also assessed the aggrecan expression in GP and AF. Similarity, compared with the control group, aggrecan expression in GP (Fig. 5A–B, F) and inner AF (Fig. 5C, D and G) of SMOi-treated mice were also markedly decreased. The loss of aggrecan expression in IDD is due in part to a decreased capacity for synthesis, and is also associated with degradation in the extracellular matrix by MMPs and aggrecanases *in vivo* [30]. MMP-13 in one of the major MMPs implicated in disc proteolytic destruction, and which is also

involved in the hypertrophic differentiation of chondrocytes in IVDs [31]. However, not as expected, IHC analysis for MMP-13 showed that the proportion of positive cells in CEP (Fig. 5H, I and L), GP (Fig. 5H, I and M) and AF (Fig. 5J, K and N) of SMOi-treated mice after 2 weeks for SMOi treatment were decreased relative to the vehicle control mice. Runx2 is widely supposed as one of the most recognized transcription factor that associated with osteoblast differentiation and chondrocytes maturation [32]. IHC results show that the proportion of Runx2 positive cells in GP and CEP of SMOi-treated mice significantly decreased relative to vehicle control mice (Fig. 6A–D). Thus, above results indicates that systemic delivery of SMOi in mice delays the terminal differentiation of chondrocytes in IVDs.

Furthermore, we investigated proliferation and apoptosis of chondrocytes in IVDs. Ki-67 protein is a marker for cellular proliferation, and the levels of Ki-67 expression is associated with cellular proliferation [33]. Terminal deoxynucleotidyl transferase dUTP nick end labeling (TUNEL) assay is a method for detecting DNA fragmentation during cellular apoptosis [34]. IHC analysis for Ki-67 revealed that there was a significantly decrease of proliferating cells in CEP (Fig. 7A, B and E), GP (Fig. 7A, B and F) and inner AF (Fig. 7C, D and G) in SMOi-treated mice. On the other hand, TUNEL-positive apoptotic cells were more abundant in CEP (Fig. 7H, I and L), GP (Fig. 7H, I and M) and inner AF (Fig. 7J, K and N) of SMOi-treated mice in comparison with control vehicle treatment mice. These data suggests that systemic delivery of SMOi in mice
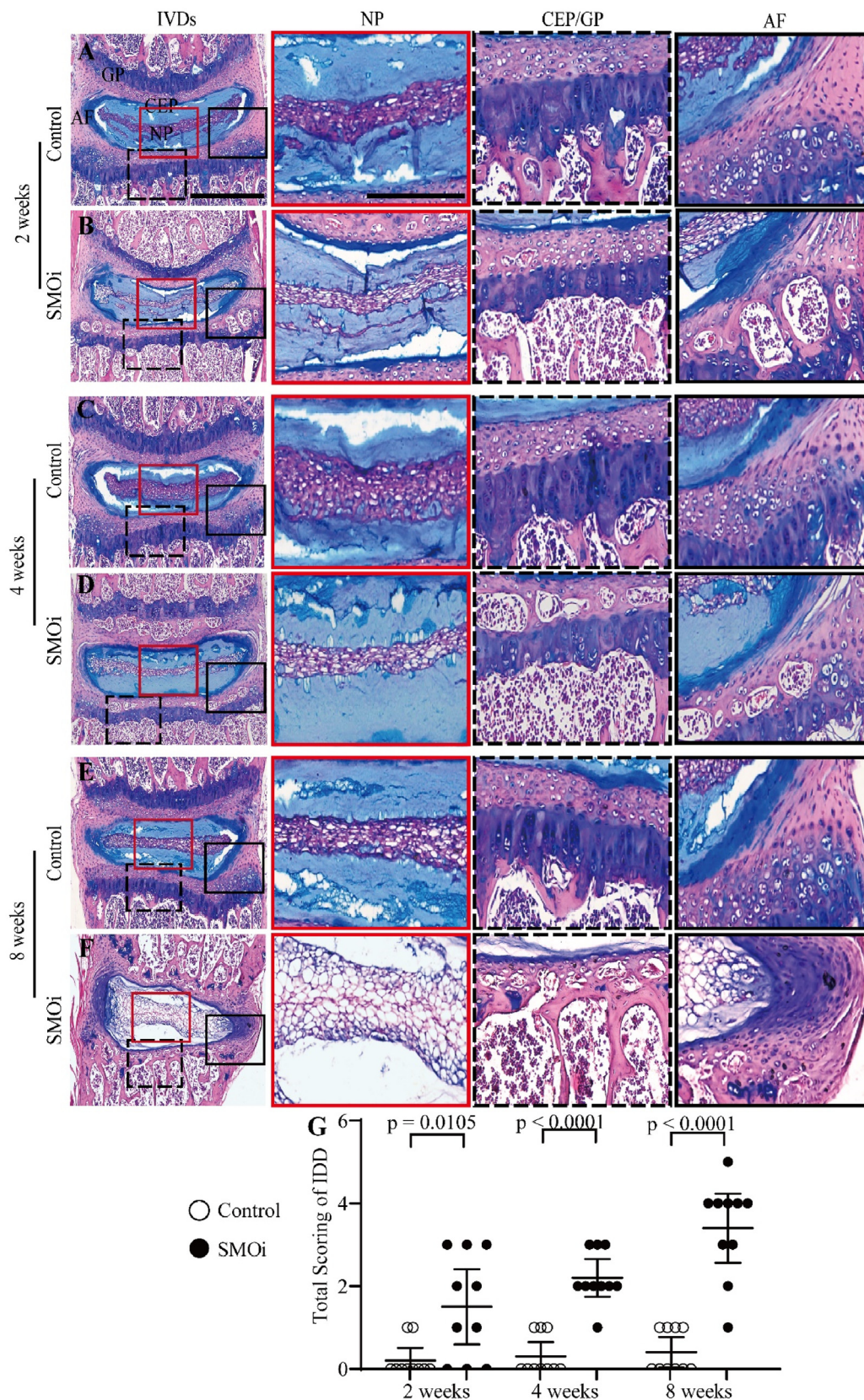
Figure 4. Histological assessment of the IVDs (L4/5) in mice. (A-F) H&E combined Alcian blue stained sections of IVDs in the SMOi and control groups and higher magnification views of NP, GP/CEP and AF shown in boxes. **(G)** Total scores of IDD in SMOi and control groups. AF: annulus fibrosus, NP: nucleus pulposus, GP: growth plates, CEP: cartilaginous endplates. SMOi: smoothened inhibitor, vismodegib. Values represent mean with 95%CI. *p < 0.05, (n = 10), Scale bar: 500 μm (**A-F**) Scale bar: 250 μm (higher magnification views).
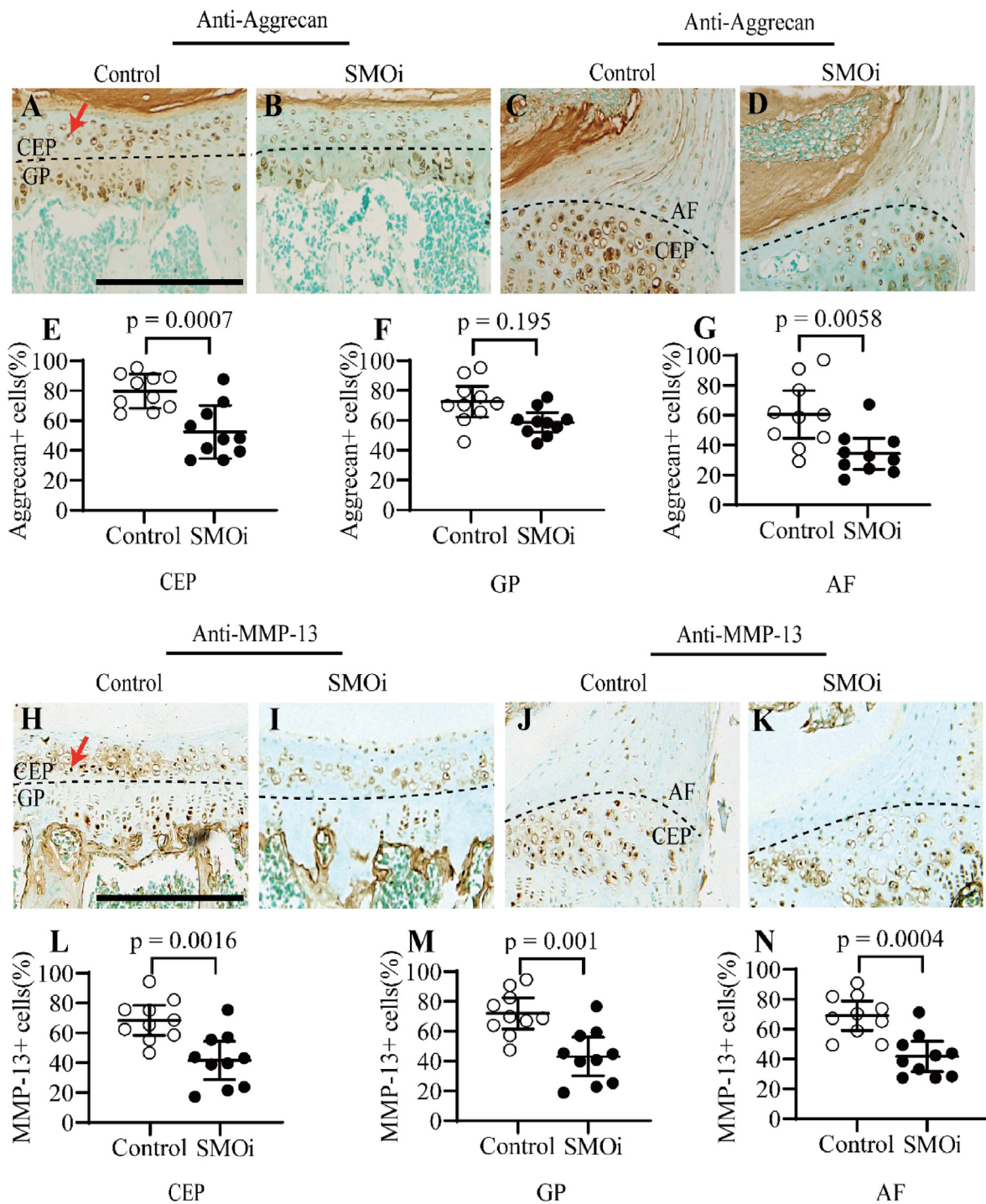
Figure 5. Immunohistochemistry assay for aggrecan and MMP-13 in IVDs of mice treated with SMOi for 2 weeks. The aggrecan-positive cells in CEP (**A, B, E**), GP (**A, B, F**) and AF (**C, D, G**) in SMOi and control groups. MMP13-positive cells in CEP (**H, I, L**), GP (**H, I, M**) and AF (**J, K, N**) in SMOi and control groups. GP: growth plates, CEP: cartilaginous endplates. SMOi: smoothened inhibitor, vismodegib. Values represent mean with 95%CI. *p < 0.05 (n = 10). Scale bar: 500 μm. Red arrows: positive cells.

inhibits the proliferation of chondrocytes in IVDs, while enhanced their apoptosis.

4. Discussion

Our data show that systemic administration of a targeted Smo inhibition (vismodegib, SMOi) damages IVDs homeostasis via inhibition of Ihh signaling in adult mice (Fig. 8). At the adult stage, the downstream of Ihh signaling, Gli1, is abundantly expressed in the tissues of IVDs.

Inhibiting Ihh signaling by targeting Smo resulted in CEP sclerosis, fissure within AF, NP degradation and loss extracellular matrix in cartilage tissues of IVDs as well as loss volume of GP and trabecular bone of vertebral bodies. These data suggest that SMOi leads IDD-like defects in IVDs of adult mice. Our further histological analysis revealed decreased cellular proliferation and increased cellular apoptosis in chondrocytes of CEP and GP after SMOi treatment. Thus, we conclude that the downregulated activation of Ihh signaling inhibits the survival of normal chondrocytes in IVDs during the adult stage.
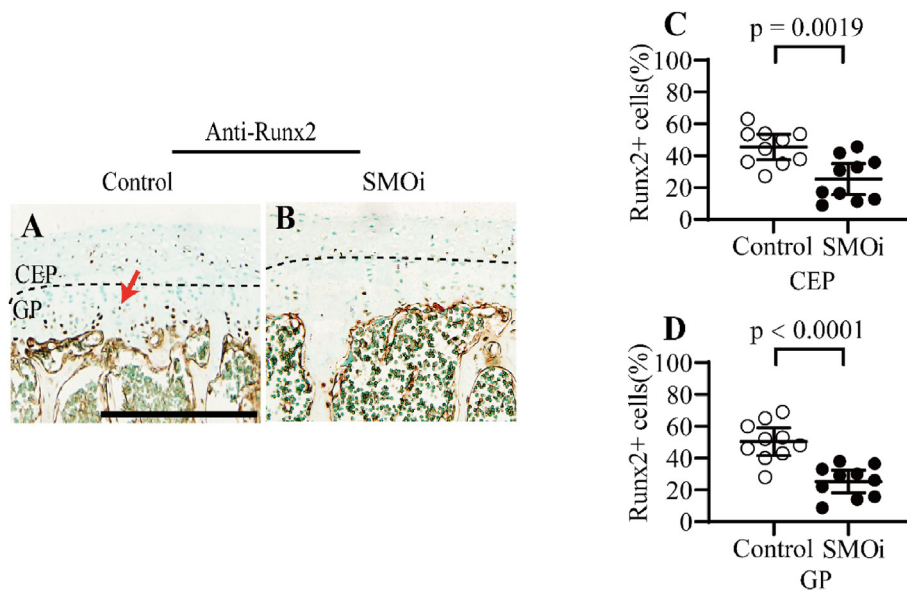
Figure 6. Immunohistochemistry assay for Runx2 in IVDs of mice treated with SMOi for 2 weeks. Runx2-positive cells in CEP and GP in SMOi and control groups. Red arrows: positive cells. GP: growth plates, CEP: cartilaginous endplates, SMOi: smoothened inhibitor, vismodegib. Values represent mean with 95%CI. *p < 0.05. (n = 10), Scale bar: 500 μm.

In our study, loss of vertebral bone was observed in mice during the adult stage after SMOi treatment. It is known that Ihh signaling is suggested to exert important role on osteoblasts differentiation and maturation to sustain trabecular bone and protect the volume and structure of trabecular bone from osteopenia [26,35,36]. Therefore, we speculate that SMOi treatment impair the volume of vertebral bone in mice at least in part via the inhibition of osteoblasts differentiation and maturation in bone remodeling. Additionally, our data showed that the loss volume of primary trabeculae under the GP was observed in mice after SMOi treatment, and the homeostasis of the GP was also disordered. Ihh signaling acts as a master regulator in endochondral ossification during GP development [37], and plays an essential role in maintaining the GP for sustaining trabecular bone during postnatal stage [36]. We suggest the possibility that both the disorder of endochondral ossification and bone remodeling abnormality are involve in the decreased volume of vertebral bone caused by the inhibition of Ihh signaling.

Bone cavities in mice after SMOi treatment were surrounded with the bone matrix, which is similar to CEP sclerosis, as one of IDD-like phenotypes, caused by the disorder of endochondral ossification reported in previous studies [28]. At the early stage of SMOi treatment, the ossification of CEP was primarily observed in outer border, and which was becoming more obvious following time. In the view of the fact that previous studies have identified IVDs progenitor cells in stem cell niche areas of IVDs located in perichondrium areas outside of the epiphyseal plate [38]. In accordance with previous reports [14], our data show that the downstream target Gli1 of Ihh signaling are expressed to different extents in all components of adult mice IVDs. Recently, it is reported that conditional ablation of Ihh in chondrocytes of adult mice led to reduce the numbers of chondroprogenitors *in vivo* [17], while activation of Ihh signaling in mesenchymal stem cells induces cartilage and bone tumor formation [39]. Thus, we speculate that Ihh signaling inhibition impairs chondroprogenitors in stem cell niche areas of IVDs, which is involved in the development of CEP ossification in our study. Additionally, CEP is the main way of nourishing IVDs. One of the important mechanisms of IDD is CEP degeneration or sclerosis which reduces nutrient supply of IVDs [40]. In some studies, CEP ossification with a reduction in porosity and permeability accelerated degeneration of IVDs during the osteoporosis process [41,42], which suggests that the disorder of vertebral bone remodeling in SMOi-treated mice may hinder the transfer of nutrients to cartilage and accelerate CEP degeneration or sclerosis.

Our further analysis revealed that the loss of aggrecan expression, as another common feature of IDD, was observed in tissues of IVDs after SMOi treatment. During the pathological process of IDD, loss of aggrecan in part be due to a decreased capacity for synthesis after the terminal differentiation of chondrocytes, and is also associated with increased extracellular matrix degradation by MMPs and aggrecanases [30]. Our data showed that the down-regulation of chondrocyte terminal differentiation and MMP13 expression in normal IVDs cartilaginous tissues of SMOi-treated mice. In fact, activation of Ihh signaling promotes the differentiation of periarticular chondrocytes into columnar chondrocytes of GP [43,44], while chondrocyte-specific inhibition of Ihh signaling delays chondrocyte hypertrophy in mice [8]. Additionally, Ihh blockade reduced the expression of MMPs and aggrecanases, including MMP13 and ADAMTS5 (a disintegrin and metalloproteinase with thrombospondin motifs), in cartilage samples of mice and human [11,12]. These evidences confirm that the decreased expression of extracellular matrix in SMOi-treated mice in our study is not mainly due to the regulation of chondrocyte differentiation and matrix catabolism by Ihh signaling. We observed the reduced proliferation and increased apoptotic incidence of chondrocytes in IVDs of SMOi-treated mice and similar findings have been present in postnatal condylar cartilage [17]. Considering that the proportion of the resident chondrocytes are closely related to the expression of aggrecan, we suggest that the downregulated activation of Ihh signaling via SMOi treatment impair the survival of normal chondrocytes in IVDs and result in the loss of extracellular matrix during the adult stage.

Previous studies reported that an aberrant activation of Ihh signaling occurred in OA chondrocytes, and which leading to cartilage degeneration [9,11]. Moreover, the protective effect of Ihh signaling inhibition was reported in surgically induced knee joint OA [12]. Thus, it is well-known that inhibiting Ihh signaling in chondrocytes as a potential therapeutic strategy can prevent and treat OA. However, this study showed that Ihh pathway inhibition caused IDD-like changes in healthy adult mice. In our previous study, the cartilage fusion of GP in long bone was observed in SMOi-treated mice, but no significant change was observed in articular cartilage of knee joints [45]. Additionally, the different effect of Ihh signaling inhibition on the different types of articular cartilage during the adult stage was reported [12,17]. We consider that the role of Ihh signaling on the cartilage degeneration due to a complex interaction with other pathological factors or the
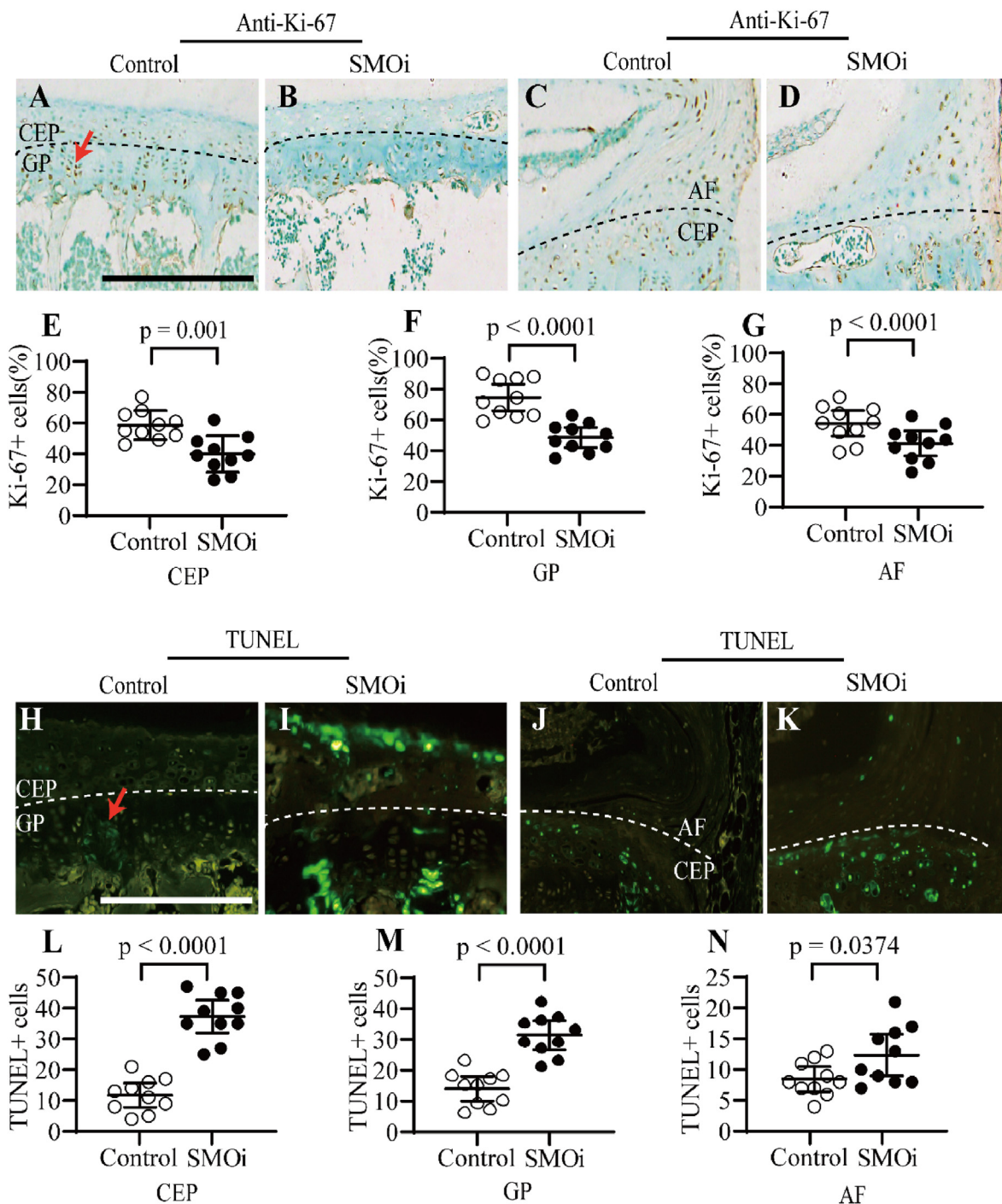
Figure 7. Immunohistochemistry for Ki-67 and TUNEL assay in IVDs of mice treated with SMOi for 2-weeks. Ki-67 positive cells in CEP (**A, B, E**), GP (**A, B, F**) and AF (**C, D, G**) in SMOi and control groups. The TUNEL-positive cells in CEP (**H, I, L**), GP (**H, I, M**) and AF (**J, K, N**) in SMOi and control groups. GP: growth plates, CEP: cartilaginous endplates, SMOi: smoothened inhibitor, vismodegib. Values represent mean with 95%CI. *p < 0.05, (n = 10). Scale bar: 500 μm.

chondrocyte fate in different cartilage tissues, such that any role of Ihh signaling is extremely context-dependent. Therefore, the clinical application of vismodegib regulating the Ihh signaling pathway needs to be particularly cautious, especially for juvenile patients with benign diseases. For example, the systematic application of vismodegib was reported to induce early epiphyseal closure in juveniles with cancers, which has received increasing attention [46–48]. To the best of our knowledge, the present study is the first to observe vismodegib causing early fusion of the metaphyseal in the vertebral body, and we further elucidate the possible mechanism that vismodegib causes IDD-like

changes, at least in part, via inhibiting proliferation of IVDs chondrocytes and promoting apoptosis to disrupt cartilage homeostasis. Certainly, the results of our study are required to be verified by more clinical studies in the future, so that we can pay attention to the long-term effect of vismodegib on skeletal system in clinical application.

However, this study has several limitations. Firstly, although the vacuolation of NP cells and loss of extracellular matrix were observed in NP tissues of SMOi groups, we did not perform immunohistochemical methods to further evaluate these changes. This is because the tissue of nucleus pulposus was obviously lost in IHC staining of paraffin sections.
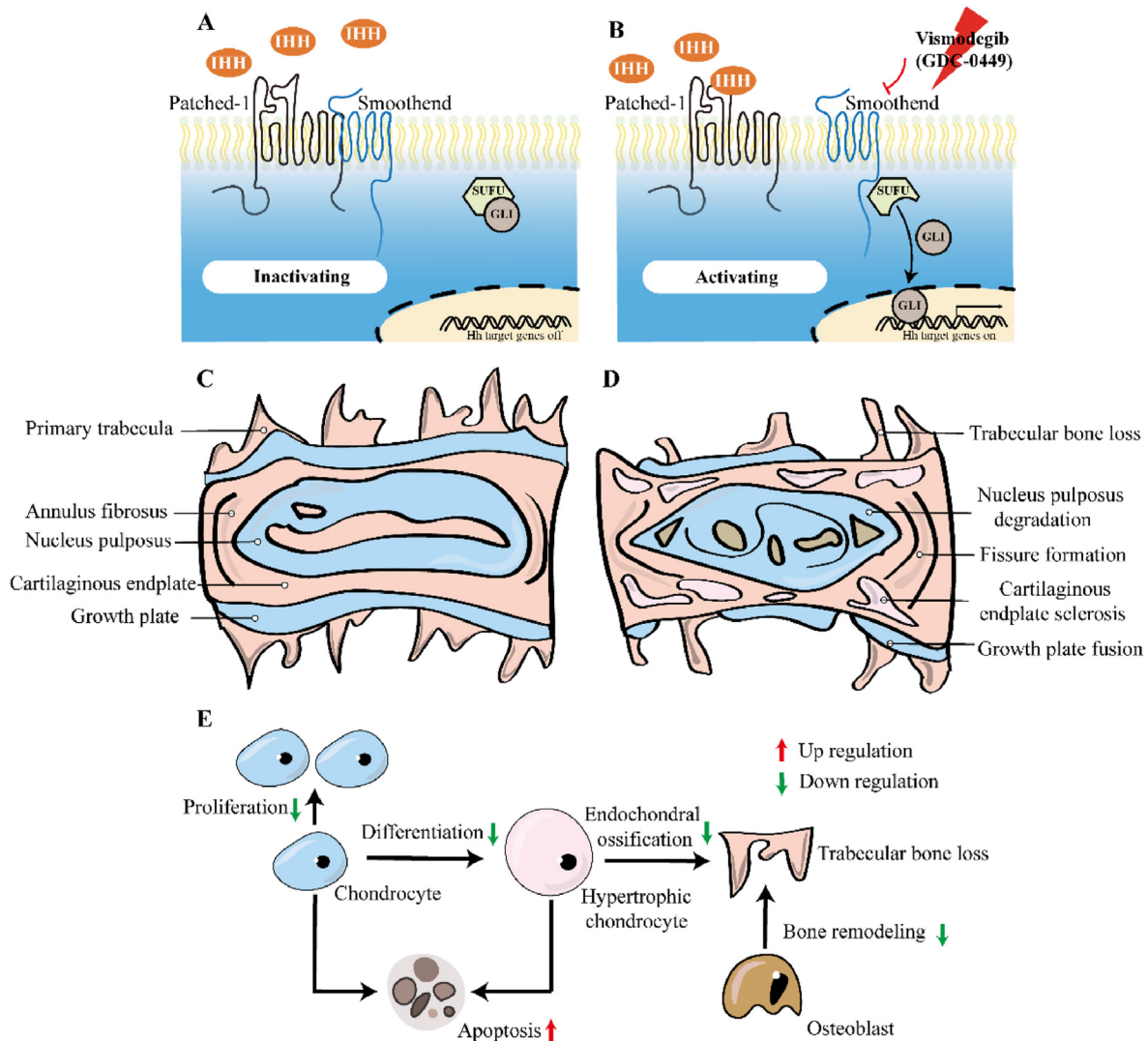
Figure 8. **Summary a targeted Smoothed inhibitor, SMOi (Vismodegib, GDC0449), damages IVDs homeostasis via inhibition of Ihh signaling in adult mice.** **(A)** Inactive Ihh signaling occurs in the absence of Ihh ligand in which receptor Pitch1 represses SMO leading to the sequestration of Gli by SUFU (Suppressor of Fused). **(B)** Active Ihh signaling occurs in the presence of Ihh ligand in which Pitch1 relieves SMO. Activated SMO promotes disassociation of Gli from SUFU, resulting in the activation of Hh target genes. SMOi (Vismodegib, GDC-0449) bound to SMO and inhibiting their combination with Gli-SUFU complex, then disturbing the release of Gli into nucleus and activation of Hh target genes. **(C)** Normal structure of the IVDs in adult mice. IVDs are composed of well-organized annulus fibrosus, nucleus pulposus and cartilaginous endplate connects them to adjacent growth plate and bony vertebrae. **(D)** Systemic administration of SMOi in adult mice results in IDD-like defects characterized by CEP sclerosis, NP degradation and fissure formation within AF, as well as GP fusion and trabecular bone loss. **(E)** Blockade of Ihh signaling pathway promotes the apoptotic activity of IVDs chondrocytes, but that inhibits their proliferation and hypertrophic differentiation. These pathological changes in the growth plate lead a decrease in endochondral ossification. Additionally, Ihh signaling inhibition impair the volume of vertebral bone in mice at least in part via the inhibition of osteoblast differentiation and maturation.

Secondly, although the results of our study, such as advanced fusion of GP, are consistent with published clinical reports, SMOi was administered to mice in our study in different doses and frequencies compared with patients, further studies should clarify the optimal timing and dosage of Ihh signaling inhibitors in clinical practice in order to improve treatment outcome and minimize the deleterious effects on different types of cartilage tissues *in vivo*. Thirdly, vismodegib was reported to regulate intracellular Ca2+ homeostasis in cisplatin-resistant lung cancer cells [49]. Although the well-defined non-specific activities of Vismodegib on cartilage tissues was not reported in previous studies, the off-target effects are difficult to avoid by using the selective inhibitor compounds of the Ihh signaling [50]. Therefore, conditional inactivation of Ihh signaling in IVD tissues during adult stages by using genetic animal model is needed to further support our conclusion in following studies.

5. Conclusion

Our study propose that systemic administration of SMOi damages IVDs homeostasis via inhibition of Ihh signaling in adult mice. The clinical application of Ihh signaling antagonists such as vismodegib should be careful considering these side adverse.

Author contributions

Z.S, C.R., T.Y., and L.Y contributed to the design of the study. C.R., T.Y., Z.S, and L.Y contributed to the acquisition, collection and assembly of data. C.R., T.Y., S.Z., Y.X., N.Z., J.H., K.L., L.X and C.H. contributed reagents/materials/analysis tools. C.R., T.Y., L.Y., and S.Z. wrote the main manuscript text. C.R., T.Y., S.Z., C.L. and L.R contributed to the revision of the manuscript. All authors contributed in revising the

manuscript and approved the final version to be submitted.

Funding

This work was supported by National Natural Science Foundation of China (No. 81802205 and No. 81830075), Chongqing foundation & Advanced Research Project Grant cstc2017jcyjAX0148 and Innovation Developing Program of Army Medical Center (2019CXJX018).

Availability of data and materials

The datasets generated/analyzed during the current study are available.

Ethics approval and consent to participate

All mice were of the C3H/HeJ background. Animal studies were performed in strict accordance with protocols approved by the Laboratory Animal Welfare and Ethics Committee of Army Medical center (Chongqing, China). The animals received humane care in accordance with the Guide for the Care and Use of Laboratory Animals published by the US National Institutes of Health and utmost care was taken to minimize the numbers and suffering of included animals.

Consent for publication

Not applicable.

Declaration of competing interest

All authors declared no potential conflicts of interest.

Acknowledgments

The authors thank Fengtao Luo and Peng Yang (Army Medical Center, Army Medical University, Chongqing, People's Republic of China) for technical support.

Appendix A. Supplementary data

Supplementary data to this article can be found online at https://doi.org/10.1016/j.jot.2022.09.009.

References

[1] Knezevic NN, Candido KD, Vlaeyen JWS, Van Zundert J, Cohen SP. Low back pain. Lancet 2021;398(10294):78–92.

[2] Lyu FJ, Cui H, Pan H, Mc Cheung K, Cao X, Iatridis JC, et al. Painful intervertebral disc degeneration and inflammation: from laboratory evidence to clinical interventions. Bone Res 2021;9(1):7 [eng].

[3] Dahia CL, Mahoney EJ, Durrani AA, Wylie C. Intercellular signaling pathways active during intervertebral disc growth, differentiation, and aging. Spine 2009;34(5):456–62 [eng].

[4] Dahia CL, Mahoney EJ, Durrani AA, Wylie C. Intercellular signaling pathways active during and after growth and differentiation of the lumbar vertebral growth plate. Spine 2011;36(14):1071–80 [eng].

[5] Carpenter RL, Ray H. Safety and tolerability of sonic hedgehog pathway inhibitors in cancer. Drug Saf 2019;42(2):263–79 [eng].

[6] Rajesh D, Dahia CL. Role of sonic hedgehog signaling pathway in intervertebral disc formation and maintenance. Curr Mol Biol Rep 2018;4(4):173–9.

[7] St-Jacques B, Hammerschmidt M, McMahon AP. Indian hedgehog signaling regulates proliferation and differentiation of chondrocytes and is essential for bone formation. Genes Dev 1999;13(16):2072–86 [eng].

[8] Mak KK, Kronenberg HM, Chuang PT, Mackem S, Yang Y. Indian hedgehog signals independently of PTHrP to promote chondrocyte hypertrophy. Development (Cambridge, England) 2008;135(11):1947–56 [eng].

[9] Wei F, Zhou J, Wei X, Zhang J, Fleming BC, Terek R, et al. Activation of Indian hedgehog promotes chondrocyte hypertrophy and upregulation of MMP-13 in human osteoarthritic cartilage. Osteoarthritis Cartilage 2012;20(7):755–63 [eng].

[10] Lu K, Ma F, Yi D, Yu H, Tong L, Chen D. Molecular signaling in temporomandibular joint osteoarthritis. J Orthop Translat 2022;32:21–7 [eng].

[11] Lin AC, Seeto BL, Bartoszko JM, Khoury MA, Whetstone H, Ho L, et al. Modulating hedgehog signaling can attenuate the severity of osteoarthritis. Nat Med 2009;15(12):1421–5 [eng].

[12] Zhou J, Chen Q, Lanske B, Fleming BC, Terek R, Wei X, et al. Disrupting the Indian hedgehog signaling pathway in vivo attenuates surgically induced osteoarthritis progression in Col2a1-CreERT2; Ihhfl/fl mice. Arthritis Res Ther 2014;16(1):R11 [eng].

[13] Rutges JP, Duit RA, Kummer JA, Oner FC, van Rijen MH, Verbout AJ, et al. Hypertrophic differentiation and calcification during intervertebral disc degeneration. Osteoarthritis Cartilage 2010;18(11):1487–95 [eng].

[14] Dahia CL, Mahoney E, Wylie C. Shh signaling from the nucleus pulposus is required for the postnatal growth and differentiation of the mouse intervertebral disc. PLoS One 2012;7(4):e35944 [eng].

[15] Wang S, Yang K, Chen S, Wang J, Du G, Fan S, et al. Indian hedgehog contributes to human cartilage endplate degeneration. Eur Spine J : Off Publ Eur Spine Soc Eur Spinal Deformity Soc Eur Sect Cervical Spine Res Soc 2015;24(8):1720–8 [eng].

[16] Zhou S, Xie Y, Li W, Huang J, Wang Z, Tang J, et al. Conditional deletion of Fgfr3 in chondrocytes leads to osteoarthritis-like defects in temporomandibular joint of adult mice. Sci Rep 2016;6:24039 [eng].

[17] Kurio N, Saunders C, Bechtold TE, Salhab I, Nah HD, Sinha S, et al. Roles of Ihh signaling in chondroprogenitor function in postnatal condylar cartilage. Matrix Biol : J Int Soc Matrix Biol 2018;67:15–31 [eng].

[18] Carpenter RL, Ray H. Safety and Tolerability of Sonic Hedgehog Pathway Inhibitors in Cancer. Drug Saf 2019;42(2):263–79.

[19] Boos N, Weissbach S, Rohrbach H, Weiler C, Spratt KF, Nerlich AG. Classification of age-related changes in lumbar intervertebral discs: 2002 Volvo Award in basic science. Spine 2002;27(23):2631–44 [eng].

[20] Masuda K, Aota Y, Muehleman C, Imai Y, Okuma M, Thonar EJ, et al. A novel rabbit model of mild, reproducible disc degeneration by an anulus needle puncture: correlation between the degree of disc injury and radiological and histological appearances of disc degeneration. Spine 2005;30(1):5–14.

[21] Melgoza IP, Chenna SS, Tessier S, Zhang Y, Tang SY, Ohnishi T, et al. Development of a standardized histopathology scoring system using machine learning algorithms for intervertebral disc degeneration in the mouse model-An ORS spine section initiative. JOR Spine 2021;4(2). e1164-e64. [eng].

[22] Avery JT, Zhang R, Boohaker RJ. GLI1: a therapeutic target for cancer. Front Oncol 2021;11:673154 [eng].

[23] Shi Y, He G, Lee WC, McKenzie JA, Silva MJ, Long F. Gli1 identifies osteogenic progenitors for bone formation and fracture repair. Nat Commun 2017;8(1):2043 [eng].

[24] Hojo H, Ohba S, Yano F, Saito T, Ikeda T, Nakajima K, et al. Gli1 protein participates in Hedgehog-mediated specification of osteoblast lineage during endochondral ossification. J Biol Chem 2012;287(21):17860–9 [eng].

[25] Rohatgi R, Milenkovic L, Scott MP. Patched1 regulates hedgehog signaling at the primary cilium. Science (New York, NY) 2007;317(5836):372–6 [eng].

[26] Lv WT, Du DH, Gao RJ, Yu CW, Jia Y, Jia ZF, et al. Regulation of hedgehog signaling offers a novel perspective for bone homeostasis disorder treatment. Int J Mol Sci 2019;20(16) [eng].

[27] Lenton K, James AW, Manu A, Brugmann SA, Birker D, Nelson ER, et al. Indian hedgehog positively regulates calvarial ossification and modulates bone morphogenetic protein signaling. Genesis (New York, NY : 2000) 2011;49(10):784–96 [eng].

[28] Bian Q, Jain A, Xu X, Kebaish K, Crane JL, Zhang Z, et al. Excessive activation of TGFβ by spinal instability causes vertebral endplate sclerosis. Sci Rep 2016;6:27093 [eng].

[29] Ling Z, Li L, Chen Y, Hu H, Zhao X, Wilson J, et al. Changes of the end plate cartilage are associated with intervertebral disc degeneration: a quantitative magnetic resonance imaging study in rhesus monkeys and humans. J Orthop Translat 2020;24:23–31 [eng].

[30] Sivan SS, Wachtel E, Roughley P. Structure, function, aging and turnover of aggrecan in the intervertebral disc. Biochim Biophys Acta 2014;1840(10):3181–9 [eng].

[31] Roughley PJ. Biology of intervertebral disc aging and degeneration: involvement of the extracellular matrix. Spine 2004;29(23):2691–9 [eng].

[32] Sato S, Kimura A, Ozdemir J, Asou Y, Miyazaki M, Jinno T, et al. The distinct role of the Runx proteins in chondrocyte differentiation and intervertebral disc degeneration: findings in murine models and in human disease. Arthritis Rheum 2008;58(9):2764–75 [eng].

[33] Sobecki M, Mrouj K, Camasses A, Parisis N, Nicolas E, Llères D, et al. The cell proliferation antigen Ki-67 organises heterochromatin. Elife 2016;5:e13722 [eng].

[34] Kyrylkova K, Kyryachenko S, Leid M, Kioussi C. Detection of apoptosis by TUNEL assay. Methods Mol Biol (Clifton, NJ) 2012;887:41–7 [eng].

[35] Rodda SJ, McMahon AP. Distinct roles for Hedgehog and canonical Wnt signaling in specification, differentiation and maintenance of osteoblast progenitors. Development (Cambridge, England) 2006;133(16):3231–44 [eng].

[36] Maeda Y, Nakamura E, Nguyen MT, Suva LJ, Swain FL, Razzaque MS, et al. Indian Hedgehog produced by postnatal chondrocytes is essential for maintaining a growth plate and trabecular bone. Proc Natl Acad Sci U S A 2007;104(15):6382–7 [eng].

[37] Ohba S. Hedgehog signaling in endochondral ossification. J Dev Biol 2016;4(2):20.

[38] Ma K, Chen S, Li Z, Deng X, Huang D, Xiong L, et al. Mechanisms of endogenous repair failure during intervertebral disc degeneration. Osteoarthritis Cartilage 2019;27(1):41–8 [eng].

[39] Deng Q, Li P, Che M, Liu J, Biswas S, Ma G, et al. Activation of hedgehog signaling in mesenchymal stem cells induces cartilage and bone tumor formation via Wnt/β-Catenin. Elife 2019;8 [eng].

[40] Urban JP, Smith S, Fairbank JC. Nutrition of the intervertebral disc. Spine 2004; 29(23):2700–9 [eng].

[41] Xiao ZF, He JB, Su GY, Chen MH, Hou Y, Chen SD, et al. Osteoporosis of the vertebra and osteochondral remodeling of the endplate causes intervertebral disc degeneration in ovariectomized mice. Arthritis Res Ther 2018;20(1):207 [eng].

[42] Ding Y, Jiang J, Zhou J, Wu X, Huang Z, Chen J, et al. The effects of osteoporosis and disc degeneration on vertebral cartilage endplate lesions in rats. Eur Spine J : Off Publ Eur Spine Soc Eur Spinal Deformity Soc Eur Sect Cervical Spine Res Soc 2014;23(9):1848–55 [eng].

[43] Kobayashi T, Chung UI, Schipani E, Starbuck M, Karsenty G, Katagiri T, et al. PTHrP and Indian hedgehog control differentiation of growth plate chondrocytes at multiple steps. Development (Cambridge, England) 2002;129(12):2977–86 [eng].

[44] Kobayashi T, Soegiarto DW, Yang Y, Lanske B, Schipani E, McMahon AP, et al. Indian hedgehog stimulates periarticular chondrocyte differentiation to regulate growth plate length independently of PTHrP. J Clin Invest 2005;115(7):1734–42 [eng].

[45] Zhou S, Xie Y, Tang J, Huang J, Huang Q, Xu W, et al. FGFR3 deficiency causes multiple chondroma-like lesions by upregulating hedgehog signaling. PLoS Genet 2015;11(6):e1005214 [eng].

[46] Robinson GW, Kaste SC, Chemaitilly W, Bowers DC, Laughton S, Smith A, et al. Irreversible growth plate fusions in children with medulloblastoma treated with a targeted hedgehog pathway inhibitor. Oncotarget 2017;8(41):69295–302.

[47] Ramesh S, Savendahl L, Madhuri V, Zaman F. Radial shock waves prevent growth retardation caused by the clinically used drug vismodegib in ex vivo cultured bones. Sci Rep 2020;10(1).

[48] Lucas Jr JT, Wright KD. Vismodegib and physeal closure in a pediatric patient. Pediatr Blood Cancer 2016;63(11). 2058-58.

[49] Tian F, Schroedl K, Kiefl R, Huber RM, Bergner A. The hedgehog pathway inhibitor GDC-0449 alters intracellular Ca2+ homeostasis and inhibits cell growth in cisplatin-resistant lung cancer cells. Anticancer Res 2012;32(1):89–94.

[50] Theunissen JW, de Sauvage FJ. Paracrine Hedgehog signaling in cancer. Cancer Res 2009;69(15):6007–10 [eng].